e-ISSN: 2805-5756

PENERBIT PRESS
UNIVERSITI TEKNOLOGI MARA

Available online at
https://jaeds.uitm.edu.my

Journal of Applied Engineering Design and Simulation 6(2) 2026, 111-129

Journal of Applied Engineering Design and Simulation

Simulation and optimisation of silica gel-water adsorption chiller for enhancing the performance of cooling system

Abdulkarim Baba Rabiu[1*], Olalekan Tajudeen Popoola[1], Mubdiu Babajide Garba[1], Sheu Ibrahim Atilola[1], Hassan Kobe Ibrahim[1]

[1]*Department of Mechanical Engineering, Faculty of Engineering and Technology, University of Ilorin, 240003, Ilorin, Kwara State, Nigeria*

ARTICLE INFO

Article history:
Received 30 March 2026
Revised 6 July 2026
Accepted 5 August 2026
Published 12 October 2026

Keywords:
Adsorption Cooling
MATLAB
Optimisation
Coefficient of Performance
Specific Cooling Capacity
Specific Cooling Power

DOI:

10.24191/jaeds.v6i2.185

ABSTRACT

The adsorption cooling system (ACS) using silica gel-water as working-fluid pair is gaining more traction as a substitute for vapor compression system (VCS) due to its environmental friendliness and low energy cost. This paper focuses on improving the efficiency of cooling processes by utilizing silica gel-water adsorption system. The MATLAB-based simulation models integrated with brute force techniques and empirical lumped analytical simulation were adopted in enhancing the operations. Three operational models (A, B, and C) were utilized, with models A and B validating the experimental setup. Model A simulates a laboratory version of a two-bed chiller which uses the Tóth equation for equilibrium uptake and the Clausius-Clapeyron relations for the pressure dynamics. Model B investigates the performance of a two-bed type adsorption chiller with different adsorbents properties. Both models were aligned with experimental outcomes, with Coefficient of Performance (COP) 0.43 and 0.55, specific cooling capacity (SCC) 74.0 and 69.7 W/kg, specific cooling power (SCP) 19.5 and 10.2 W/kg, across hot water (70 to 80°C) and chilled water (-4 to 20°C). The Mean Absolute Percentage Error (MAPE) was between 2.47 to 4.19%, while the Mean Absolute Error (MAE) was between 0.014 to 0.022. Model C enables predictive analysis via user-defined inputs (adsorbent mass, flow rates and temperatures), employing parallel processing for parametric sweeps and transient phase-switching dynamics. Results highlight the system's adaptability to low-grade heat (70 to 80°C, typical of solar thermal or industrial waste heat) and at subzero temperatures, emphasizing its potential for diverse applications. The computational rigor of the framework is validated through thermodynamic and kinetic accuracy, demonstrating silica gel-water adsorption viability in reducing electricity demand and greenhouse emissions. The findings are

[1*]Corresponding author. E-mail address: rabiu.br@unilorin.edu.ng

beneficial to designers of ACS system using silica gel-water as a working-fluid pair, thus contributing to sustainable solutions, which are aligned with global decarbonization goals.

Nomenclature (Greek symbols towards the end)

A	area of heat exchanger (m^2)
CC	cooling capacity (W)
COP	coefficient of performance
SCC	specific cooling capacity (W/kg)
SCP	specific cooling power (W/kg)
c_p	specific heat capacity at constant pressure ($kJ/kg°C$)
$\frac{dM_{chilled}}{dt}$	mass flow rate of chilled water (kg/s)
$\frac{dM_{cooling}}{dt}$	mass flow rate of cooling water (kg/s)
$\frac{dM_{heating}}{dt}$	mass flow rate of hot water (kg/s)
D_s	diffusive surface (m^2/s)
D_{so}	water-silica gel kinetic diffusion constant (m^2/s)
E_a	activation energy ($kJ/kmol$)
h	specific enthalpy (kJ/kg)
HP	heating power with the hot water flow (W)
K	mass transfer coefficient (kW/mK)
K_o	Tóth constant
M	mass (kg)
n	structural heterogeneity parameter
P	pressure (Pa)
q	amount of vapor adsorbed in the bed (kg/kg)
q^*	maximum bed saturation under given temperature and pressure (kg/kg)
q^o	monolayer maximum adsorption capacity (kg/kg)
Q_{st}	isosteric heat of adsorption (kJ/kg)
R	individual or universal gas constant ($kJ/kmol°C$)
R_p	average radius of silica-gel particles (m)
t	time (s)
T	temperature (°C)
T_o	temperature at starting point (°C)
$tcycle$	cycle time (s)
T_k	temperature of water in heat exchanger (°C)
U_{cond}	heat transfer coefficient during condensation ($W/m^2°C$)
$U_{cooling}$	heat transfer coefficient during bed cooling ($W/m^2°C$)
U_{evap}	heat transfer coefficient during evaporation ($W/m^2°C$)
$U_{heating}$	heat transfer coefficient during bed heating ($W/m^2°C$)
γ	flag coefficient
δ	flag coefficient
θ	flag coefficient
ρ	density of water at a given temperature (kg/m^3)
χ	flag coefficient

Abbreviations

ads	Adsorber
bed	Bed
chw	chilled water
$cond$	Condenser
cw	cooling water
$evap$	Evaporator
f	liquid state
g	gas, vapour state
Hex	heat exchanger
hw	hot water
i	Inlet
ini	initial state
max	Maximum
o	Outlet
ref	Refrigerant
s	saturated state
sg	silica gel
x	Adsorption
y	Desorption
z	switching time

1. INTRODUCTION

The unceasing global increase in population and human aspiration for a better standard of living from one generation to another has consistently driven high demand for sustainable solutions that bring about comfort, affluence, and safety. In order to ensure environmental sustainability, several policies and pacts had been endorsed by countries around the world, among these is the adoption of Vienna Convention of 1985 [1-2]. This convention was directed towards the protection of ozone layer from depletion, which later played significant roles during the establishment of Montreal Protocol in 1987 [3-4]. During the meeting, seventy-five (75) countries and development partners agreed to focus on the reduction of ozone-depleting anthropogenic chemicals such as chlorine and bromine [5-6] in various applications.

The scientific perspective concluded that the protection of ozone layer requires phasing-out substances currently controlled under the Protocol, and replace them with more environmentally friendly substances [7]. The refrigerants (fluorine-based) in recent refrigeration systems account for over 50% of the chlorofluorocarbon emission released into the atmosphere [8]. However, this global strive to protect the ecosystem and its habitants has paved ways for more studies on the exploration of environmentally friendly refrigerants for cooling and heating systems. In recent times, the emergence of renewed interests in the development and optimization of cooling system technology keeps increasing in order to address global concerns of climate change and public health challenges.

The escalating demand for sustainable and efficient cooling technologies has prompted the exploration of alternative solutions to curtail greenhouse gas emissions and mitigate climate change effects [9-10], [11-13]. Adsorption refrigeration systems have also emerged as a promising substitute for traditional vapor compression systems [14], offering distinct advantages such as diminished negative environmental impact,

heightened efficiency, and compatibility with low grade or residual heat sources [6], [15-17]. Adsorption refrigeration systems function by adsorbing a refrigerant into a solid adsorbent substance that has high affinity with it, followed by desorption to induce cooling [8, 18]. Among these systems, the silica gel-water adsorption chiller has attracted significant interest, and remains the focus of extensive research and development [19].

The overall performance of silica-gel adsorption chiller can be analysed using some thermodynamic parameters, particularly the specific cooling capacity (SCC) and specific cooling power (SCP). The amount of cooling energy produced per unit mass of the adsorbent during adsorption/desorption cycle is referred to as specific cooling capacity, while the rate of useful cooling produce per unit mass of the absorbent is specific cooling power. However, the SCP demonstrates practical performance and compactness of the adsorption chiller. Variations of adsorption and desorption temperatures, condenser and evaporator temperatures, overall system pressure, time requires to complete a cycle, and the equilibrium pattern of the adsorption system working fluid-pair may influence both SCC and SCP. These parameters are quite significant in the evaluation and determination of process condition and optimising capacities of the adsorption refrigeration system.

Adsorption refrigeration system is typically known with some practical limitations, which include relatively low specific cooling power (SCP) compared to vapor compression systems, a large system footprint per unit cooling capacity, intermittent operation that necessitates thermal storage or auxiliary heating, and reduced performance at elevated condenser temperatures [6]. At the same time, they present strong opportunities for development, particularly through integration with solar thermal collectors, recovery of low-grade industrial waste heat below 100°C, hybridization with vapor compression cycles, and deployment in off-grid or remote areas where electricity access is limited. These prospects provide the motivation for the present optimization effort.

Theoretical and experimental studies in recent years have focused on the performance of adsorption chillers employing different heat generation sources such as solar energy source, industrial and commercial waste heat, fossil fuel-source, geothermal energy source, biomass fuel systems and nuclear fission. The profound attentions to the exploration of adsorption/desorption refrigeration system have manifested into numerous theoretical and experimental studies aimed at enhancing performance and optimization. Leveraging simulation methodologies and advanced optimization techniques, such as genetic algorithms, holds the potential to substantially augment the efficiency and reliability of these systems [20]. Through persistent research and development endeavours, the application outlook for silica gel and water adsorption chillers appears promising across diverse cooling and refrigeration applications [21-22]. However, most existing studies are limited to lab-scale systems with fixed operating parameters, leaving critical questions unanswered regarding optimal control strategies under variable heat source conditions, performance at subzero chilled water temperatures, and the development of user-customizable predictive frameworks that can adapt to different adsorbent masses, flow rates, and temperature ranges.

Several experimental studies have characterized silica gel-water adsorption chillers. For instance, Chen et al. [23] performed experimental study on performance change with time of solar adsorption refrigeration system using SAPO-34 zeolite and water as working pair. The result of their work established that the adsorption rate initially increases with adsorption bed temperature attaining a maximum COP of 0.133. Afterward, the adsorption rate decreases with gradual drop in bed temperature, which resulted in

performance deterioration of the system and poor heat and mass transfer of the adsorber. Their work laid more emphasis on inefficiency caused due to poor heat and mass transfer phenomenon during the operation.

Pan et al. [24] presented a comprehensive thermal design of a small-scale silica gel-water adsorption chiller with heat and mass recovery scheme with the mind of a performance test below solar water temperature of 70°C. The results of their work showed that COP was able to reach a value of 0.385 while SCP attained 140.3 W/kg. Results also showed that increasing the cooling water inlet temperature from 26°C to 32°C resulted in 11.2 and 28.9% reduction of COP and SCP, whilst increasing the chilled water inlet temperature led to a 61.1% and 114.1% increment of COP and SCP, respectively. However, this study was limited to lab-scale systems with fixed cycle times, leaving questions about optimal control under variable heat source conditions.

Du et al. [25] worked on a compact silica gel-water adsorption chiller for waste heat driven cooling in data centres. The developed adsorption chiller was able to achieve a cooling power of 4.9 kW and COP of 0.50 with hot water inlet temperature, cooling inlet temperature and chilled water inlet temperature of 50°C, 30°C and 23°C respectively. With cooling water inlet temperature changing from 32°C to 24°C, cooling power and COP increased to between 3.04 kW to 10.50 kW and 0.44 to 0.66 respectively. However, the research work was limited to small modular data centre and low driving temperatures.

Abdullah et al. [26] evaluated solar adsorption cooling systems using economic, environmental, and energy indices, demonstrating that annual energy costs can be reduced by up to 74% compared to conventional vapor compression systems, with maximum theoretical COP of 0.5 and SCP of 102 W/kg at a regeneration temperature of approximately 127℃. Koushaeian et al. [19] investigated hybrid adsorption-compression refrigeration systems by integrating silica gel within a compression refrigeration cycle in cascade mode. Their hybrid model showed that there was 58.87% reduction in electrical power consumption when compared to vapor compression chiller for 15 kW cooling load. They were able to demonstrate that when hot water temperature increased from 70°C to 90°C, there was a higher refrigerant mass in the adsorption chiller unit, resulting in 44.59% increase of overall COP and 7.33% reduction of energy consumption. Despite these advances, few studies have systematically optimized operating parameters across a wide range of boundary conditions.

Numerical modelling has been widely employed to predict and optimize chiller performance. Liu et al. [22] developed a thermodynamic model for a silica gel-water adsorption chiller and employed a genetic algorithm to optimize desorption temperature and coolant flow, achieving significant COP improvements. Lemington et al. [18] implemented a transient MATLAB simulation to determine temperature profiles, reporting COP values between 0.043 and 0.342. While these studies demonstrated the utility of simulation, they either focused on single-objective optimization or lacked experimental validation across a wide range of chilled water temperatures. Despite progress in modelling and experimentation, no existing study has provided a validated, user-customizable simulation framework that combines, rigorous validation against two independent experimental datasets, parametric sweeps to identify optimal operating zones across broad temperature ranges (including subzero chilled water), and predictive capability for user-defined inputs (adsorbent mass, flow rates, temperatures).

The current paper aims to develop a thermodynamic simulation framework to predict and optimize the operational performance of a two-bed silica gel-water adsorption chiller under variable heat source and chilled water conditions. The framework is implemented in MATLAB to enable parametric sweeps, transient cycle analysis, and user-defined scenario testing. The work is in alignment with broader goals of advancing sustainable and energy-efficient cooling technologies, addressing environmental concerns, and maximizing energy utilization efficiency. To relate the performance evaluation in a real-world cooling demand scenario, this study adopts typical atmospheric conditions in Lagos, Nigeria, a region with high cooling load, limited grid reliability, and significant solar resource potential. The adoption of Lagos residential conditions, therefore, serves to address this gap by providing a real-world reference for SCP assessment in typical residential settings, particularly relevant for hot-climate, developing-economy applications.

2. METHODOLOGY

2.1. Descriptions of the physical model

Figure 1 illustrates the schematic representation of the simulated configuration of the two-bed silica gel-water adsorption chillers. Within this arrangement, each adsorbent bed was either connected to the condenser or evaporator using flap valves. These valves responded to the pressure differences between the heat exchangers during the adsorption or desorption phases, allowing them to open or close accordingly. Furthermore, the control of heating and cooling water flow across the heat exchangers was facilitated by a set of 8 pneumatic valves.

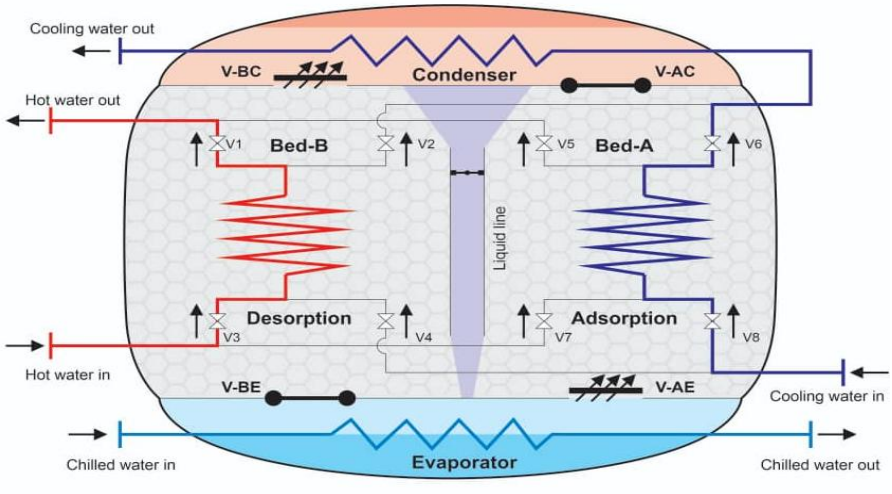


Fig. 1. Schematic Representation of Simulated Two-bed Adsorption Chiller

2.2. Mathematical Model

2.2.1. Energy balance during adsorption phase

The energy balance link with the condenser (index x) for the bed can be obtained using equation (1):

$$\begin{aligned}&\left(M_{sg}cp_{sg}+M_{Hex}cp_{Hex}\right.\\&\left.+M_{sg}q_{bed,x}\left[cp_{sg}T_{bed,x}+Q_{st}\left\{\frac{1}{T_{bed,x}}-\frac{1}{V_gT_{bed,x}}\left(\frac{\partial V_g}{\partial T_{bed,x}}\right)\right\}\right]\right)\frac{dT_{bed,x}}{dt}\\&=M_{sg}\frac{dT_{bed,x}}{dt}\left[\delta\left\{h_g\left(T_{i,cw}\right)-h_{g(Tbed,x)}+Q_{st}\right\}+(1-\delta)\left\{h_g\left(T_{evap}\right)-h_g(T_{bed,x})+Q_{st}\right\}\right]\\&-U_{cooling,}A_{bed,x}(T_{bed,x}-T_k)\end{aligned} \quad \text{(W)} \qquad (1)$$

2.2.2. Energy Balance During Desorption Phase

The energy balance link with the condenser for the bed (index y) is defined by equation (2):

$$\begin{aligned}&\left(M_{sg}cp_{sg}+M_{Hex}cp_{Hex}\right.\\&\left.+M_{sg}q_{bed,y}\left[cp_{sg}T_{bed,y}+Q_{st}\left\{\frac{1}{T_{bed,y}}-\frac{1}{V_gT_{bed,y}}\left(\frac{\partial V_g}{\partial T_{bed,y}}\right)\right\}\right](+)\right)\frac{dT_{bed,y}}{dt}\\&=M_{sg}\frac{dT_{bed,y}}{dt}\left[\theta\left\{h_g\left(T_{i,hw}\right)-h_{g(Tbed,y)}+Q_{st}\right\}+(1-\theta)\left\{h_g(T_{cond})-h_g(T_{bed,y})+Q_{st}\right\}\right]\\&-U_{heating,}A_{bed,y}(T_{bed,y}-T_k)\end{aligned} \quad \text{(W)} \qquad (2)$$

2.2.3. Energy balance for the evaporator

The evaporator energy balance is given by equation (3):

$$\begin{aligned}&\left[cp_f\left(T_{evap}\right)M_{ref,evap}+cp_{evap}M_{evap}\right]\frac{dT_{evap}}{dt}+h_f\left(T_{evap}\right)\frac{dM_{ref,evap}}{dt}\\&=-\theta(1-\gamma)h_f(T_{cond})M_{sg}\frac{dq_{bed,x}}{dt}-\left[\delta h_g(T_{evap})+(1-\delta)h_g(T_{bed,x})\right]M_{sg}\frac{dq_{bed,x}}{dt}\\&-U_{evap}A_{evap}\left(T_{evap}-T_k\right)\end{aligned} \quad \text{(W)} \qquad (3)$$

2.2.4. Energy balance for the condenser

The energy balance of condenser can be obtained by the following equation (4):

$$\begin{aligned}&\left[cp_f(T_{cond})M_{ref,cond}+cp_{cond}M_{cond}\right]\frac{dT_{cond}}{dt}+h_f(T_{cond})\frac{dq_{bed,y}}{dt}\\&=-\left[\theta h_g(T_{bed,y})+(1-\theta)h_g(T_{cond})-\theta(1-\gamma)h_f(T_{cond})\right]M_{sg}\frac{dq_{bed,y}}{dt}\\&-U_{cond}A_{cond}(T_{cond}-T_k)\end{aligned} \quad \text{(W)} \qquad (4)$$

The adsorption isotherms used in the simulation were based on the research conducted by Wang et al. [27]. This study investigated the isotherm of silica gel-water systems using thermogravimetric and volumetric methods. Additionally, Elsheniti et al. [20] developed a correlation for the major adsorption isotherm and found that Tóth isotherm is the most suitable for this experimental model, which was earlier affirmed by the comprehensive study of Chua et al. [28] that assessed isotherm models for silica gel-water systems with Tóth model, demonstrating the lowest average absolute deviation from the experimental values. The Tóth isotherm and the constant parameters are given in Equation (5) and Table 1.

$$q^* = \frac{K_o \, exp\left(\frac{\Delta H_{ads}}{RT}\right) p}{\left[1 + \left(\frac{K_o}{q_m} exp(\frac{\Delta H_{ads}}{RT}) p\right)^t\right]^{1/t}} \quad \text{(kg/kg)} \qquad (5)$$

Table 1. Tóth equation parameters

Parameter	Value	Unit
K_O	1.92E-02	[kg/ kg(kPa)]
ΔH_{ads}	2.72E + 03	[kJ/kg]
q_m	0.38	[kg/kg]
T	8.7	-

2.3. Performance Indicator

The mass of air in an average Lagos Nigerian home is considered to determine the Specific Cooling Power (SCP) of the System, which is given by;

$$M_{air} = \text{Density}_{air} \times \text{Volume}_{air} \quad \text{(kg)} \qquad (6)$$

The average yearly temperature of 27°C for Lagos, Nigeria was adopted from the work of Olorunmaiye et al. (2012) which was used to determine the density of 1.176 kg/m^3 for the air in the room and the room average area of 4.5 m^2 and a height of 2.7 m [29]. The average volume of air was taken as 12.15 m^3 since air occupies all spaces. This gives the mass of air as 14.29 kg. However, the evaluation of Specific Cooling Power (SCP) was not considered in the experimental reviews used for simulation validation (Model A and Model B).

The Coefficient of Performance (COP), which was determined by Rezk and Al-Dadah (2012), is given in equations 7 to 10 [30]:

$$Q_{chilled} = \frac{\int_0^{tcycle} M_{chilled} \, cp_{f,i,chw}(T_{i,chw} - T_{o,chw})}{t_{cycle}} \quad \text{(W)} \qquad (7)$$

$$Q_{hot} = \frac{\int_0^{tcucle} M_{heating} cp_{f,i,hw}(T_{i,hw} - T_{o,hw})}{t_{cycle}} \quad \text{(W)} \qquad (8)$$

$$Q_{net} = Q_{hot} - Q_{chilled} \quad \text{(W)} \qquad (9)$$

$$COP = \frac{Q_{chilled}}{Q_{hot}} \tag{10}$$

The SCC and SCP are the specific cooling capacity and specific cooling power achieved by the system, respectively. The HPR is the heat pumping rate supplied by the system. The SCC, SCP and HPR can be determined from equations (11), (12) and (13), respectively.

$$SCC = \frac{Q_{chilled}}{M_{ads}} \quad (\mathrm{W/kg}) \tag{11}$$

$$SCP = \frac{Q_{chilled}}{M_{air}} \quad (\mathrm{W/kg}) \tag{12}$$

$$HPR = \frac{Q_{net}}{M_{ads}} \quad (\mathrm{W/kg}) \tag{13}$$

2.4. Simulation

The simulation of the adsorption system model was formulated by integrating four distinct sub-models, each detailing the behaviour of the condenser, evaporator, adsorbed, and desorbed components. These four sub-models were interconnected, considering the array of operational modes. Accordingly, the energy balance equations governing the adsorbent bed, evaporator, and condenser were outlined in equation 1 to equation 4 [30]. These set of equations were modified and utilized in a compact form in the simulation program whose framework was developed to systematically analyse adsorption chiller performance across three distinct operational models. Models A and B were designed to rigorously validate experimental studies, while Model C enabled predictive analysis through user-customizable inputs. To achieve this, the methodology integrated parametric sweeps, time-series simulations, and validation protocols to holistically assess thermodynamic and kinetic behaviour.

Model A was implemented as a foundational step to replicate the lab-scale two-bed adsorption chiller described by Elsheniti et al. (2018) [20]. Specifically, parameters from the referenced study (Table 2), including adsorbent mass, equilibrium constants, and cycle times, were systematically integrated. Key governing equations, such as the Tóth equation for equilibrium uptake and the Clausius-Clapeyron relation for pressure-temperature dynamics, formed the computational backbone. To validate reproducibility, parametric sweeps generated COP and SCC values across hot (70 to 80°C) and chilled (10 to 20°C) water temperature ranges, with results cross-verified against experimental data via mean absolute percentage error MAPE and MAE.

Building on this foundation, Model B focused on validating adsorption kinetics under low-grade heat conditions [31]. Here, adjusted mass transfer coefficients and silica gel properties (Table 3) were incorporated, with extended cycle times (4,800 s) accounting for slower intraparticle diffusion in crushed silica gel. Notably, the Tóth isotherm equation was adapted to model non-isothermal adsorption, and performance metrics were evaluated across broader chilled water temperatures (−4 to 15°C). To ensure consistency, error metrics (MAPE, MAE) were computed by directly comparing simulated COP and SCC against experimental values under identical boundary conditions.

Model C introduced a customizable and efficient framework for predictive analysis, allowing user-defined inputs with built-in validation to ensure physical consistency. An integrated validation module assesses accuracy by comparing simulated and experimental results using metrics such as MAPE and MAE, supported by visualization tools for clear interpretation. Additionally, multidimensional plots, including surface, contour, and time-series representations, enable comprehensive analysis of system performance and identification of optimal operating conditions.

The governing Ordinary Differential Equations (1) - (4) were solved using a fixed-step explicit Euler scheme (Δt = 1 s) in a custom MATLAB script. Initial conditions assumed fully regenerated beds (q = 0 kg/kg) at cooling water temperature (25-30°C). Phase switching (adsorption/precool/desorption/ preheat) was controlled by a state machine with user-defined durations. Equilibrium uptake was calculated using either the Tóth or Dubinin-Astakhov isotherm, selected by the user. A linear driving force model (k = 0.01 s^{-1}) governed mass transfer, with thermodynamic properties from the Antoine equation and XSteam toolbox (IAPWS-IF97).

3. RESULTS AND DISCUSSION

The current analysis was validated using experimental data from Elsheniti et al. [20] (Model A) and Vodianitskaia et al. [31] (Model B). The governing equations (1) to (13) were simulated using MATLAB, which made it possible to accurately calculate temperature distributions and important performance metrics as COP, SCP, SCC, and HPR. To investigate the system's optimal performance, operational conditions were established and a brute-force optimization procedure was used in the validation experiment. Additionally, Tóth's isotherm provided the parameters for the lumped-mathematical model in Table 1.

Figures 2 and 3 compare the modelling and experimental results for the coefficient of performance (COP). The simulation result was within $\pm 10\%$ of experimental values under identical operating conditions, meeting conventional tolerances for adsorption chiller model validation. This comparison approach was applied since it represents a stringent test of model fidelity, as it requires simultaneous accuracy across multiple coupled thermodynamic outputs [32].

Table 2. Operating parameters used in the study of Model A

Parameters	Temperature °C	Mass flow rate (kg/s)	Other
Hot water inlet (desorber)	75	0.2533	-
Chilled water inlet (Evaporator)	14	0.1367	-
Cooling water inlet (absorber)	25	0.2533	-
Cooling water inlet (Condenser)	25	-	-
Mass of silica gel (per bed) [kg]	-	-	3.8
Switching time [s]	-	-	60
Cycle time adsorption/desorption [s]	-	-	600

Table 3. Operating parameters used in the study of Model B

Parameters	Temperature °C	Mass flow rate (kg/s)	Other
Hot water inlet (desorber)	80	0.225	-
Chilled water inlet (Evaporator)	15	0.053	-
Cooling water inlet (absorber)	30	0.25	-
Cooling water inlet (Condenser)	30	-	-
Mass of silica gel (per bed) [kg]	-	-	2.1
Switching time [s]	-	-	600
Cycle time adsorption/desorption [s]	-	-	300/1200

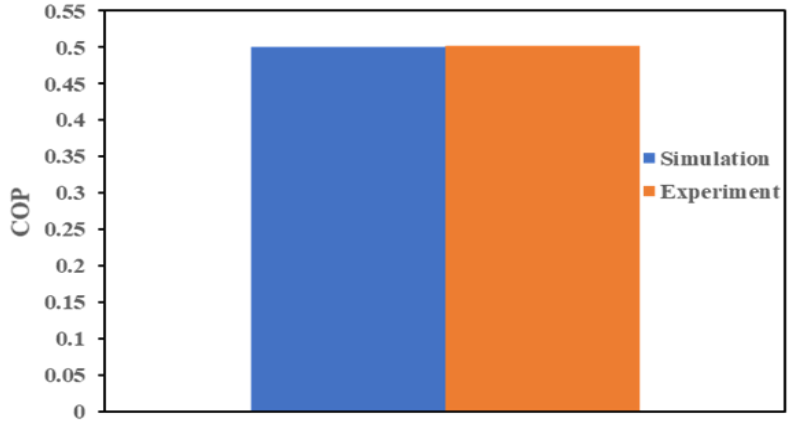


Fig. 2. Comparison between Simulated and Experimental COP Model A

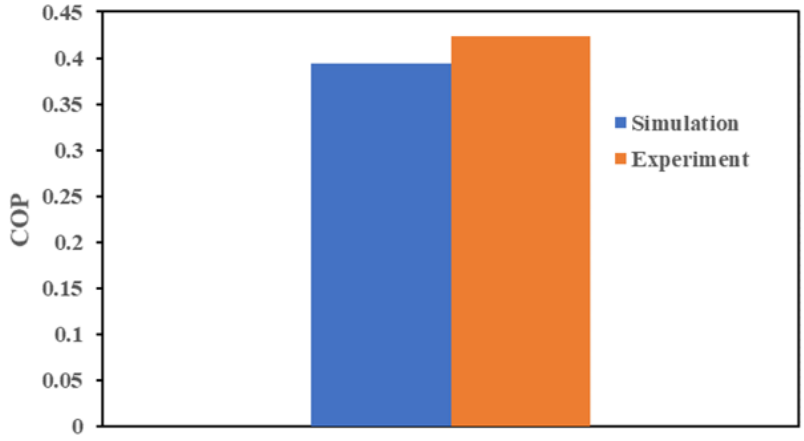


Fig 3. Comparison between Simulated and Experimental COP Model B

Table 4 presents the MAPE and MAE whose equations are highlighted below as equations 14 and 15, for the Coefficient of performance of the simulated models (A and B). The predictive value of both models is within the accepted range of ±30% for MAPE [33].

$$MAPE = \left(\frac{1}{n}\sum_{i=1}^{n}\frac{|actual - prediction|}{actual}\right) \times 100 \quad (\%) \qquad (14)$$

$$MAE = \frac{1}{n}\sum_{i=1}^{n}|actual - prediction| \qquad (15)$$

Table 4. Simulation model deviation analysis

Term	MAPE (%)	MAE
COP Model A	2.47	0.014
COP Model B	4.19	0.022

3.1. Adsorption-desorption dynamics and cycle functionality

The adsorption–desorption dynamics exhibited expected behaviour, with an initially high adsorption rate driven by strong potential gradients, followed by a gradual decline as equilibrium approached. Symmetry between the two beds confirmed balanced cycle operation. Cumulative heat transfer analysis showed a steady increase in desorption heat input (Q_{hot}), while the cooling effect (Q_{chill}) increased at a slower rate, reflecting system inefficiencies. These trends are consistent with experimental observations, supporting the validity of the simulation model.

3.2. Analysis of simulation and experimental performance at matching operating conditions

The adsorption performance of a two-bed silica gel-water chiller was evaluated through simulation under experimental benchmark conditions ($T_{I,hw}$= 75 °C, $T_{I,cw}$ = 18 °C), with results compared to empirical data from the work of Elsheniti et al. [20]. The simulation yielded a COP (0.4304), SCC (73.997 W/kg, SCP (19.5 W/kg), and heating power rate (HPR) of 653.5 W. These outcomes align closely with experimental values (COP = 0.42, SCC = 75 W/kg, SCP = 23 W/kg, HPR = 678.6 W), as quantified by mean absolute percentage errors (MAPE) of 2.47%, 1.34%, 15.10%, and 3.72%, respectively. The analysis of Figures 1 to 4 contextualizes these findings and their implications for sustainable cooling systems.

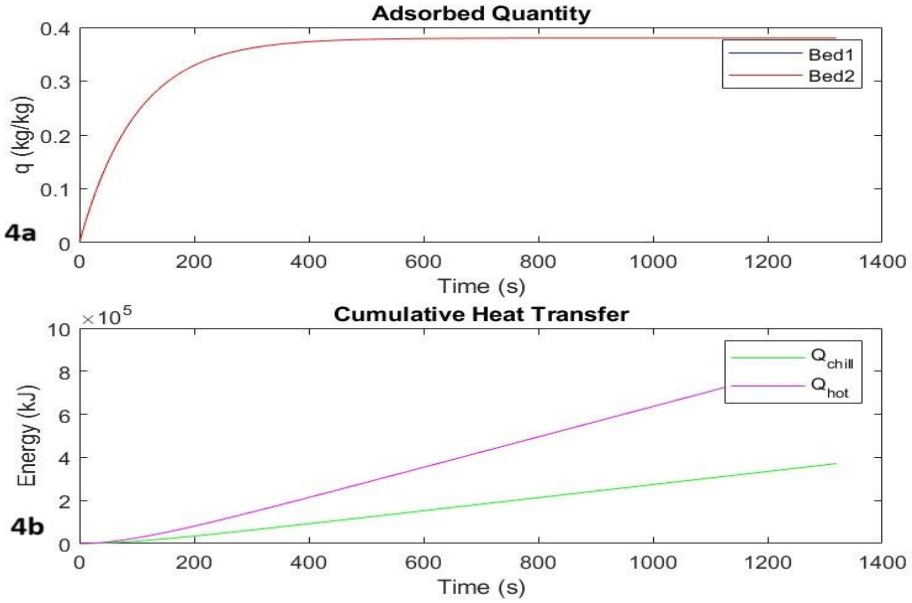


Fig. 4. Adsorption Dynamics and Cumulative Heat Transfer Analysis

3.3. Coefficient of Performance (COP)

The simulated COP of 0.4304 and 0.55 in model A and B closely matches the experimental values (MAPE of 2.47% and 4.19%), demonstrating the robustness of the model representation of energy efficiency under moderate heat input (70 to 80° C). Figure 5 illustrates the COP trend which reflects the balance between desorption kinetics and sensible heat losses. Minor deviations arise from idealized heat transfer assumptions in the model, such as uniform bed temperature distribution and negligible losses. By isolating these factors, simulations enable targeted improvements, such as enhancing bed insulation or integrating regenerative heating to elevate COP in real-world systems. For solar-driven applications, even marginal COP gains translate to significant reductions in collector area and energy waste, thereby advancing low-carbon cooling solutions.

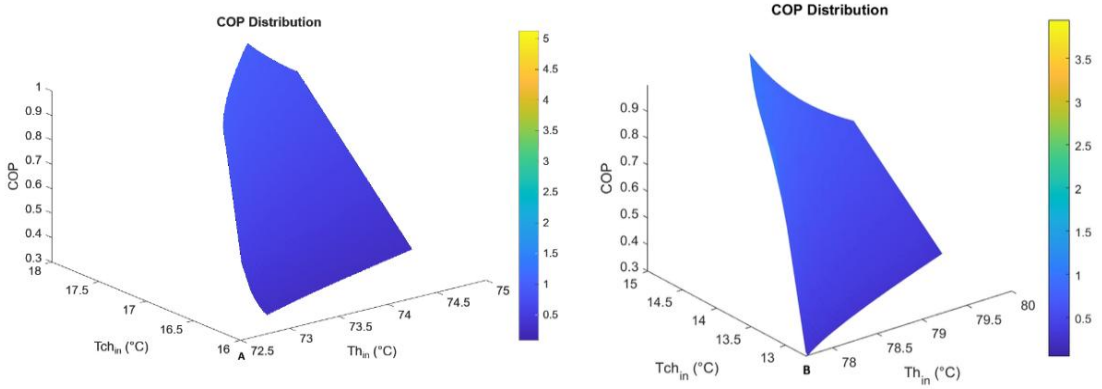


Fig.5. Effect of Water Inlet Temperature on COP

3.4. Specific Cooling Capacity (SCC)

The SCC simulation result of 73.997 W/kg and 69.7 W/kg (MAPE = 1.34% and 2.46%) closely mirrors the experimental values of 75 W/kg and 68 W/kg respectively for both models (A and B), reflecting precise modelling of adsorption kinetics and evaporation pressure dynamics. Figure 6 highlights the near-linear relationship between $T_{l,cw}$ and SCC, emphasizing the model's capability to predict cooling output under varying chilled water temperatures. Discrepancies arise from conservative assumptions in vapor pressure gradients and adsorbent porosity, which can be refined using real-world silica gel particle size distributions. Simulations at this level of accuracy allow engineers to explore SCC enhancements, such as optimizing evaporator geometry or adsorbent bed configurations without costly prototyping, accelerating the deployment of efficient and scalable chillers.

3.5. Specific Cooling Power (SCP)

The SCP simulation result of 19.5 W/kg in Model A exhibited a larger deviation from the experimental 23 W/kg (MAPE = 15.10%), attributed to oversimplified mass transfer assumptions. Meanwhile, Model B of 10.2 W/kg (MAPE = 2.45%) with experimental value of 9.92 W/kg stayed within the desired range. Figure 7 underscores the transient SCP profile, where rapid initial adsorption transitions to saturation-driven decay. Real-world systems using crushed silica gel (0.15 – 0.5 mm) experience reduced permeability and thermal conductivity, slowing adsorption kinetics. These factors are underrepresented in the model. Addressing this gap requires integrating granular particle dynamics, such as variable

intraparticle diffusivity (ζ_{eff}) and bed porosity (ε), into simulations. Improved SCP predictions would guide the design of compact high-power-density chillers capable of competing with conventional vapor-compression systems, particularly in space-constrained applications like residential cooling or electric vehicle climate control. Figure 7 shows the effect of water inlet temperature on SCP.

3.6. Heating Power Rate (HPR)

The simulated HPR of 653.5 W and 269.9 W (MAPE = 3.72% and 1.65%) aligned closely with the experimental 678.6 W and 269.4 W of Model A and B respectively, validating the model's representation of desorption energy demands. Figure 8 depicts the HPR stabilization above 75°C, indicating thermodynamic equilibrium where additional heat input yields diminishing returns. The marginal underprediction stems from excluded minor losses, such as imperfect thermal contact between silica gel and the finned tubes. Refining the model to incorporate transient heat recovery mechanisms such as phase-specific heating or advanced heat exchanger geometries could reduce HPR by 10–15%, lowering energy consumption in solar and waste heat applications. The strong agreement between simulation and experiment (MAPE ≤ 4.19% for COP, SCC, and HPR) confirms model reliability and reduces reliance on iterative prototyping. The model accurately predicts COP (Figure 5) and SCC (Figure 6), while SCP trends (Figure 7) highlight mass transfer improvements and HPR trends (Figure 8) guide heat recovery. Parametric optimization of inlet temperature $T_{I,hw}$ and $T_{I,cw}$could reduce material requirements by 15–20%, improving affordability. Overall, the model supports integration of renewable heat sources and reduction of energy use and emissions.

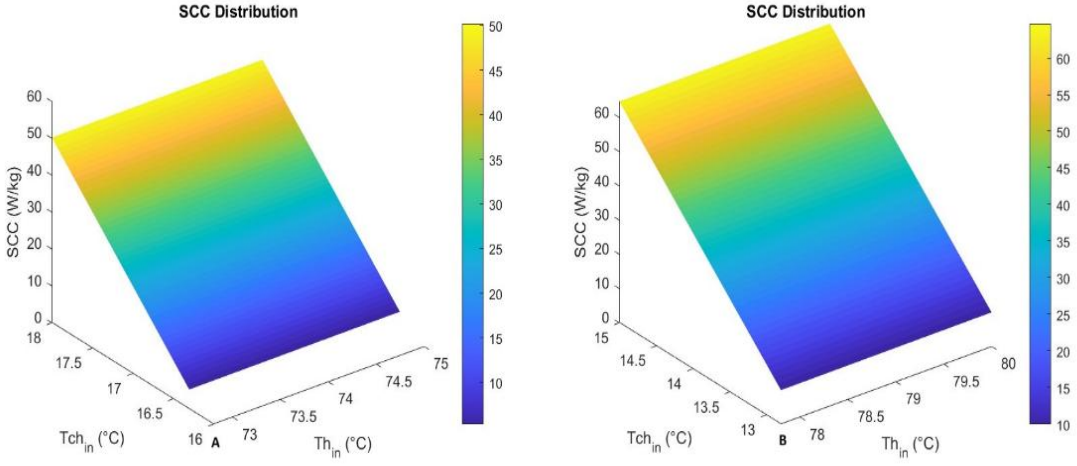


Fig. 6.Effect of Water Inlet Temperature on SCC

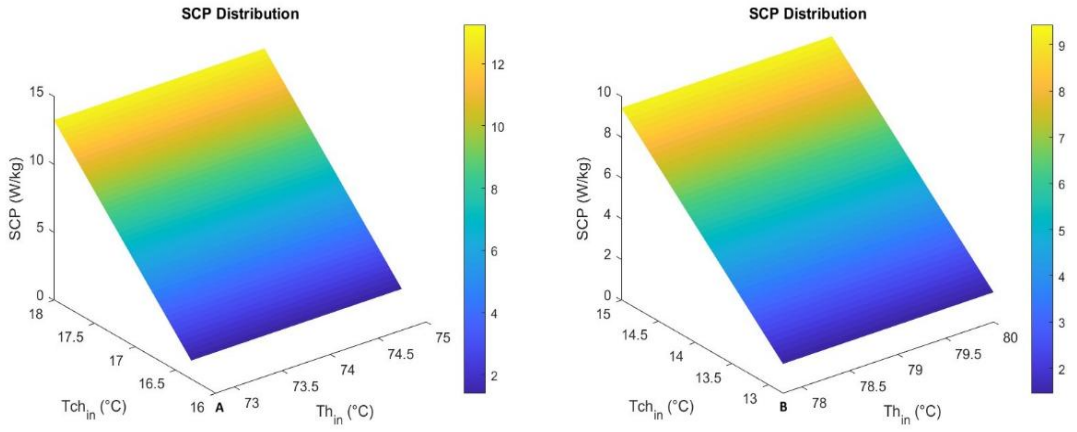


Fig. 7. Effect of Water Inlet Temperature on SCP

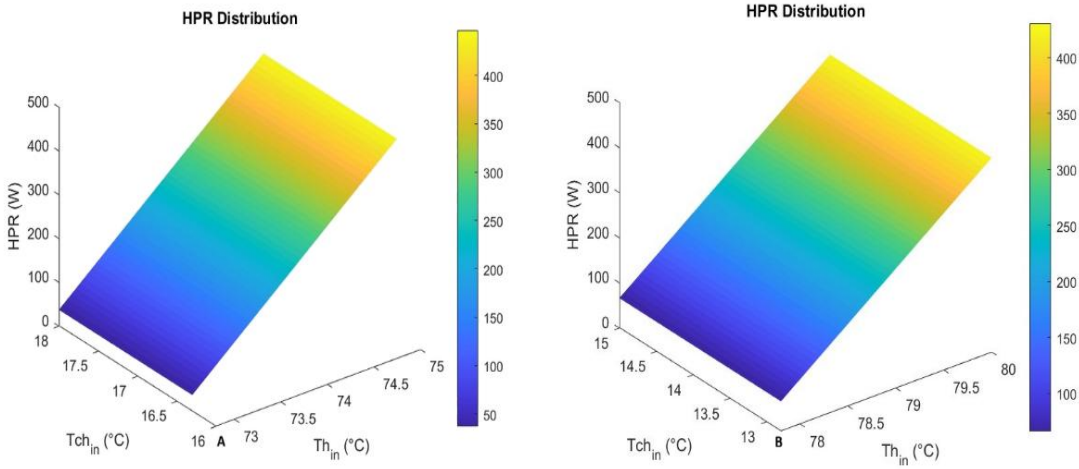


Fig. 8. Effect of Water Inlet Temperature on HPR

3.7. Effect of inlet hot water temperature ($T_{I,hw}$)

Increasing $T_{I,hw}$ enhances desorption kinetics but intensifies sensible heat losses, leading to a decline in COP (Figure 5). For instance, at $T_{I,hw} = 75$ ℃, $T_{I,cw} = 18$ ℃ and $T_{I,hw} = 80$ ℃, $T_{I,cw} = 15$ ℃, the simulated COP of both models aligned with experimental values within a 15% deviation. Beyond this value, COP remained significantly constant due to silica gel's adsorption equilibrium, where additional heat input no longer improved desorption efficiency. Concurrently, HPR raised linearly with $T_{I,hw}$ (Figure 8), reaching 653.5 W at $T_{I,hw} = 75$ ℃, while in Model A, higher temperatures demanded greater thermal energy to sustain desorption. Meanwhile, elevated $T_{I,hw}$ marginally improved SCC and SCP by accelerating

refrigerant release, and the energy requirement outweighed these benefits, necessitating a balance between desorption efficacy and operational costs.

3.8. Effect of inlet chilled water temperature ($T_{I,cw}$)

Increasing $T_{I,cw}$ enhances the evaporation pressure gradient, improving SCC and SCP as shown in Figures 6 and 7. At $T_{I,hw}$ = 75 °C, raising $T_{I,cw}$ from 14 °C to 18 °C increased SCC from 68 to 73.997 W/kg and SCP from 17.5 to 19.5 W/kg, with similar trends observed in Model B. This improvement is due to stronger adsorption driving forces, although $T_{I,cw}$ must remain below $T_{I,hw}$for effective heat rejection. The simulated SCC agreed with experimental data within 15%, confirming model reliability. However, SCP deviation (19.5 W/kg vs. 23 W/kg experimental) indicated unaccounted mass transfer limitations in silica gel beds.The interplay between $T_{I,hw}$ and $T_{I,cw}$ underscores the importance of temperature optimization. Operating at this conditioned state achieved a balanced COP (0.43 and 0.55) and SCC (74 W/kg and 69.7 W/kg), minimizing energy waste while maintaining cooling output. For regions like Nigeria, where access to affordable cooling is critical, this configuration leverages solar thermal or industrial waste heat ($T_{i,hw}$ = 70 ºC – 80 ºC), mitigating reliance on grid electricity and synthetic refrigerants. The predictive accuracy of the model (within 15% of experimental data) enables cost-effective design adoptions, cutting operational expenses by 10% to 15% through the implementation of the heat recovery strategies.

4. CONCLUSION

This study developed and validated a thermodynamic simulation framework for a two-bed silica gel-water adsorption chiller. The model showed strong agreement with two independent experimental datasets, both confirming its predictive reliability. The results demonstrate that increasing chilled water inlet temperature $T_{I,cw}$ enhances COP, SCC, and SCP, while increasing hot water inlet temperature $T_{I,hw}$ beyond the critical temperature (73.7 °C in Model A and 79.6 °C in Model B) yields diminishing returns due to sensible heat losses and adsorption equilibrium limitations. In this study, the term "critical temperature" refers to the optimal hot water inlet temperature at which the system COP peaks and beyond which no further improvement occurs. This is due to three compounding effects, including the silica gel bed approaching desorption saturation, excess heat accumulating in the adsorption beds, and the silica gel-water adsorption isotherm flattening at elevated temperatures. Both models achieved maximum COP values of 1.2 (Model A) and 1.1044 (Model B) at their respective critical temperatures (73.7 °C and 79.6 °C). The difference in critical temperature between the two models arises from variations in bed mass (3.8 kg vs. 2.1 kg), cycle timing (600 s vs. 3000/1200 s), and silica gel properties between the two experimental setups being validated. The validated Model C provides a user-friendly, customizable tool for predictive analysis, allowing engineers to explore design variations without costly prototyping. This framework supports the design of energy-efficient, low-emission cooling systems utilizing solar thermal or industrial waste heat (70°C to 80°C), particularly relevant for regions with high cooling demand and limited grid infrastructure.

5. ACKNOWLEDGEMENTS

The authors sincerely acknowledge the support provided by the Tertiary Education Trust Fund (TETFund), Nigeria, which made this research work possible. We are grateful for the funding and institutional support received through TETFund, which without could have made this study difficult to accomplish. The TETFund's commitment towards promoting research, innovation, and academic development in Nigeria is well acknowledged.

6. CONFLICT OF INTEREST STATEMENT

The authors declare that the manuscript has not been published elsewhere and is not under consideration in other journal outlets. All authors have approved the review, agreed with its submission and declare no conflict of interest with the manuscript.

7. AUTHORS' CONTRIBUTIONS

Abdulkarim Baba Rabiu: Conceptualisation of ideas, methodology, funding acquisition, and validations;

Olalekan Tajudeen Popoola: Data curation, formal analysis and resources, and software supervision;

Mubdiu Babajide Garba: Data curation, methodology, writing-review, and editing;

Sheu Ibrahim Atilola: Investigation, writing-original draft, and proof-reading; and

Hassan Kobe Ibrahim: Project administration, organisation of tasks, and supervision

8. DECLARATION OF GENERATIVE AI IN THE WRITING PROCESS

During the preparation of this work the authors used Claude (Anthropic) and DeepSeek AI to enhance the report readability and the code base development. Thereafter, the authors thoroughly reviewed and edited the contents as required and take full responsibility for the contents of the publication.

9. DATA AVAILABILITY/SUPPLEMENTARY MATERIALS

The codes use for the study are available from the corresponding authors on request.

10. ETHICAL STATEMENT

The authors declare that this research did not involve human or animal subjects. All experimental procedures were performed following the institutional health, safety and environmental (HSE) protocols of University of Ilorin, Ilorin, Nigeria.

11. REFERENCES

[1] B. Z. Umbetbayeva, S. Zh Suleimenova, S., Baitukayeva, D., A Saimova, and G. G Nurakhmetova, "The Vienna Convention for the protection of the ozone layer and its role in promoting environmental sustainability and implementation in the national legislations of participating states," 2023.

[2] M. Faure and J. Lefevere, "Compliance with international environmental agreements. In The Global Environment," in *The Global Environment*, 1st ed., N. J.Vig and R. S. Axelrod, Eds., London: Routledge, 2023, ch. 7, pp. 138–156. 1oi: https://doi.org/10.4324/9781003421368-9

[3] T. Kaniye-Ebeku, C. O., Odumosu, "The assessment of the Vienna convention for the protection of the ozone layer depletion," *J. Priv. Prop. Law*, vol. 24, no. 1, pp. 239–256, 2026.

[4] S. Guggisberg and M. Lennan, "Non-use of the Atmosphere and the Success Story of the Montreal Protocol," in *Non-use Measures for Global Goods and Commons in International Law*, 1st ed., Solène Guggisberg and C. Blanchard, Eds., Brill / Nijhoff, 2025, ch. 17, pp. 395–427. doi: https://doi.org/10.1163/9789004730571_018

[5] T. Demura and Z.-H. Ye, "Regulation of plant biomass production," *Curr. Opin. Plant Biol.*, vol. 13, no. 3, pp. 298–303, 2010, doi: https://doi.org/10.1016/j.pbi.2010.03.002.

[6] P. Soni and V. K. Gaba, "Performance analysis of adsorption refrigeration system using silicagel/methanol pair: experimental & analytical approaches," *J. Therm. Eng.*, vol. 7, no. 5, pp. 1079–1089, 2021.

[7] A. K. Vuppaladadiyam *et al.*, "Progress in the development and use of refrigerants and unintended environmental consequences," *Sci. Total Environ.*, vol. 823, p. 153670, 2022, doi: https://doi.org/10.1016/j.scitotenv.2022.153670.

[8] J.-K. Choi, A. Paudel, B. Karki, K. Bradley, N. Quinn, and A. Ciric, "Comprehensive reviews on technological and life cycle environmental aspects of solar–thermal adsorption refrigerator," *Resour. Environ. Sustain.*, vol. 19, p. 100195, 2025, doi: https://doi.org/10.1016/j.resenv.2025.100195.

[9] D. Barton, "An overview of the sustainability of emerging energy technologies in mitigating climate change," *Futur. Sustain.*, vol. 3, no. 3, pp. 35–46, 2025.

[10] A. Erdoğdu, F. Dayi, A. Yanik, F. Yildiz, and F. Ganji, "Innovative solutions for combating climate change: Advancing sustainable energy and consumption practices for a greener future," *Sustainability*, vol. 17, no. 6, p. 2697, 2025. doi: https://doi.org/10.3390/su17062697

[11] N. Ghilen, S. Messai, S. Gabsi, and B. Mohammed, El Ganaoui, Riad, "Performance Simulation of Two-Bed Silica Gel-Water Adsorption Chillers," *Glob. J. Res. Eng.*, vol. 17, no. 3, pp. 40–49, 2017.

[12] X. Wang, Z. He, and H. T. Chua, "Performance simulation of multi-bed silica gel-water adsorption chillers," *Int. J. Refrig.*, vol. 52, pp. 32–41, 2015, doi: https://doi.org/10.1016/j.ijrefrig.2014.12.016.

[13] K. H. D. Tang, "Urban solutions to climate change: An overview of latest progress," *Acad. Environ. Sci. Sustain.*, vol. 1, no. 2, 2024.

[14] S. K. Singh, D. Rakshit, K. R. Kumar, and A. Agarwal, "Recent advancements and sustainable solutions in adsorption-based cooling systems integrated with renewable energy sources and industrial waste heat: A review," *Clean. Eng. Technol.*, vol. 23, p. 100827, 2024, doi: https://doi.org/10.1016/j.clet.2024.100827.

[15] S. Vasta, "Adsorption Air-Conditioning for Automotive Applications: A Critical Review," *Energies*, vol. 16, no. 14, p. 5382, 2023. doi: https://doi.org/10.3390/en16145382

[16] M. P. Islam and T. Morimoto, "Thermodynamic performances of a solar driven adsorption system," *Sol. Energy*, vol. 139, pp. 266–277, 2016, doi: https://doi.org/10.1016/j.solener.2016.09.003.

[17] M. Kılıç, "Evaluation of combined thermal–mechanical compression systems: a review for energy efficient sustainable cooling," *Sustainability*, vol. 14, no. 21, p. 13724, 2022. doi: https://doi.org/10.3390/su142113724

[18] N. Lemington, L. Lemington, D. Budiman, M. I. Alhamid, and S. Sholahudin, "Study of solar driven adsorption cooling potential in Indonesia," *J. Therm. Eng.*, vol. 3, no. 1, pp. 1044–1051, 2017. doi: https://doi.org/10.18186/thermal.290257

[19] M. Koushaeian *et al.*, "Investigation of the cascade type of hybrid adsorption-vapor compression chiller," *Case Stud. Therm. Eng.*, vol. 47, p. 103037, 2023, doi: https://doi.org/10.1016/j.csite.2023.103037.

[20] M. B. Elsheniti, O. A. Elsamni, R. K. Al-dadah, S. Mahmoud, E. Elsayed, and K. Saleh, "Adsorption Refrigeration Technologies," in *Sustainable Air Conditioning Systems*, C. Ghenai and T. Salameh, Eds., Rijeka: IntechOpen, 2018, ch. 4. doi: 10.5772/intechopen.73167.

[21] P. R. Chauhan, S. C. Kaushik, and S. K. Tyagi, "Current status and technological advancements in adsorption refrigeration systems: A review," *Renew. Sustain. Energy Rev.*, vol. 154, p. 111808, 2022, doi: https://doi.org/10.1016/j.rser.2021.111808.

[22] Y. M. Liu, Z. X. Yuan, X. Wen, and C. X. Du, "Evaluation on performance of solar adsorption cooling of silica gel and SAPO-34 zeolite," *Appl. Therm. Eng.*, vol. 182, p. 116019, 2021, doi: https://doi.org/10.1016/j.applthermaleng.2020.116019.

[23] Q. F. Chen, S. W. Du, Z. X. Yuan, T. B. Sun, and Y. X. Li, "Experimental study on performance change with time of solar adsorption refrigeration system," *Appl. Therm. Eng.*, vol. 138, pp. 386–393, 2018, doi: https://doi.org/10.1016/j.applthermaleng.2018.04.061.

[24] Q. W. Pan, L. Liu, B. Wang, J. Xu, and T. S. Ge, "Design and experimental study on a small-scale silica gel/water adsorption chiller with heat and mass recovery scheme for solar energy use," *Sol. Energy*, vol. 252, pp. 91–100, 2023.

[25] S. Du, Z. Cui, R. Z. Wang, H. Wang, and Q. Pan, "Development and experimental study of a compact silica gel-water adsorption chiller for waste heat driven cooling in data centers," *Energy Convers. Manag.*, vol. 300, p. 117985, 2024.

[26] F. Abdullah, Ahmed Bawazir Daniel, "Evaluation and Design of Large-Scale Solar Adsorption Cooling Systems Based on Energetic, Economic and Environmental Performance," *Energies*, vol. 15, no. 6, pp. 1–24, 2022.

[27] X. Wang, W. Zimmermann, K. C. Ng, A. Chakraboty, and J. U. Keller, "Investigation on the isotherm of silica gel+water systems," *J. Therm. Anal. Calorim.*, vol. 76, no. 2, pp. 659–669, 2004, doi: 10.1023/B:JTAN.0000028045.96239.7e.

[28] H. T. Chua, K. C. Ng, A. Chakraborty, N. M. Oo, and M. A. Othman, "Adsorption characteristics of silica gel+ water systems," *J. Chem. Eng. Data*, vol. 47, no. 5, pp. 1177–1181, 2002.

[29] J. A. Olorunmaiye, K. R. Ajao, and I. S. Omolehin, "Effect of Climate Change on Outside Air Design Temperature for Air Conditioning Cooling Load Calculations For Ikeja and Ilorin, Nigeria," *Energy Eng.*, vol. 109, no. 2, pp. 65–79, 2012. doi: https://doi.org/10.1080/01998595.2012.10483747

[30] A. R. M. Rezk and R. K. Al-Dadah, "Physical and operating conditions effects on silica gel/water adsorption chiller performance," *Appl. Energy*, vol. 89, no. 1, pp. 142–149, 2012, doi: https://doi.org/10.1016/j.apenergy.2010.11.021.

[31] P. J. Vodianitskaia, J. J. Soares, H. Melo, and J. M. Gurgel, "Experimental chiller with silica gel: Adsorption kinetics analysis and performance evaluation," *Energy Convers. Manag.*, vol. 132, pp. 172–179, 2017, doi: https://doi.org/10.1016/j.enconman.2016.11.028.

[32] J. Krzywański, M. Szyc, W. Nowak, and Z. Kolenda, "Experience in modelling of a single-stage silical gel-water adsorption chiller," *Tech. Sci.*, vol. 19, no. 4, pp. 367–386, 2016.

[33] L. M. Chamra and P. J. Mago, "Modeling of condensation heat transfer of refrigerant mixture in micro-fin tubes," *Int. J. Heat Mass Transf.*, vol. 49, no. 11, pp. 1915–1921, 2006, doi: https://doi.org/10.1016/j.ijheatmasstransfer.2005.11.006

© 2026 by the authors. Submitted for possible open access publication under the terms and conditions of the Creative Commons Attribution (CC BY-NC-ND) license (http://creativecommons.org/licenses/by/4.0/).